Project Description

1 Introduction

Spurred by the need for compact & broadband telecommunications systems, detection of hazardous materials, and non-invasive medical imaging, interest in the TeraHertz (THz) portion of the electromagnetic spectrum has grown dramatically over the past few years. One major impediment to the practical realization of THz technology is the limited availability of continuous wave signal sources. Such sources are needed, for example, in the vast majority of THz receivers and transmitters. The two most widely used signal sources at THz frequencies are far-infrared (FIR) lasers and solid state frequency multipliers. The FIR laser is capable of producing milliwatts of power, but only at specific frequencies determined by the molecular structure of the lasing gas and the mid-infrared pump laser. Recent advances in solid-state frequency multiplier technology has pushed their upper frequency limit to just over 2 THz. However, at these frequencies multipliers can produce harmonics with only a few nanowatts of power. **A breakthrough in the availability of tunable THz sources is needed for the true potential of this spectral regime to be realized.**

Here we propose to conduct a series of experiments to demonstrate 1) the use of the Smith-Purcell (SP) effect to generate coherent THz radiation and 2) a traveling-wave tube (TWT) amplifier capable of operating at THz frequencies. These investigations will utilize a modified scanning electron microscope (SEM) as a convenient source of $\sim$30 keV electrons required for these experiments. The work is part of an ongoing collaboration between the University of Arizona and Raytheon Inc. to develop technologies that will help realize the potential of this important spectral regime.

2 Device Theory and Operation

2.1 Smith-Purcell Radiation

Smith-Purcell radiation is produced when an energetic electron beam passes over a conductive, periodic structure (e.g. a diffraction grating) at a fixed distance close to the surface. The effect was first predicted by Frank (1942) and observed at visible wavelengths by Smith and Purcell (1953). In their work Smith and Purcell utilized a 250-300 keV electron beam. The Coulomb field of the electrons in the beam induce currents in the underlying periodic conducting structure. The oscillating currents generate a dipole moment on the grating surface that gives rise to the observed radiation.

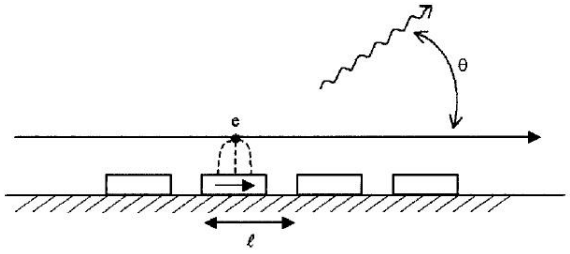

Figure 1: *Schematic representation of the Smith-Purcell (SP) effect, edited from Kube (2003).*

The generation of SP radiation is illustrated in Figure 1, where the diffraction grating is approximated by a series of narrow conducting strips on a flat plane. An

electron passing overhead induces an oscillating image current on the grating surface. The frequency (or wavelength) of the emitted radiation is set by the periodicity of the grating (D) and the electron's velocity ($\beta = v_o/c$). To the observer the perceived grating periodicity will be a function of viewing angle, hence the observed wavelength of SP radiation is a function of viewing angle. A figure illustrating SP emission from a 3-D grating is shown in Figure 2.

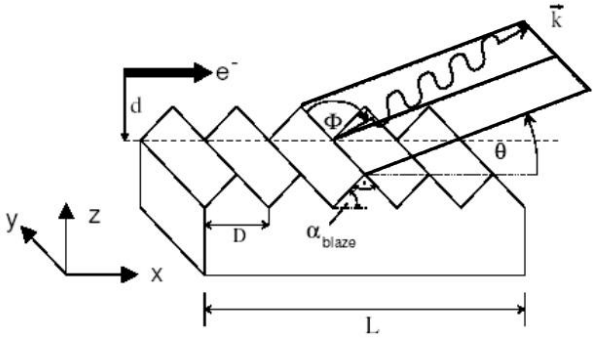

Figure 2: *Schematic representation of the Smith-Purcell (SP) effect from a 3-D grating.*

The wavelength of the SP radiation can be expressed in terms of the grating equation (Smith & Purcell 1953) as:

$$\lambda = \frac{D}{|n|}\left(1/\beta - \cos\theta\ \sin\phi\right). \qquad (1)$$

where λ is the wavelength of the emitted radiation, D is the grating period, n is the diffraction order, $\beta = v/c$ is the reduced electron velocity, and ϕ & θ are the emission angles defined in Figure 2.

The wavelength dependence of THz SP radiation has been experimentally verified by Urata et al.(1998) at THz frequencies for a variety of grating periods and beam voltages (ex. Figure 3).

The angular distribution of the emitted radiation is given by Francia (1960):

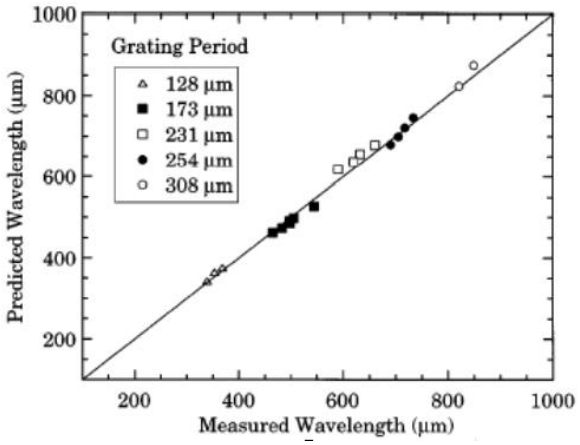

Figure 3: *Verification of the Smith-Purcell effect in dependence of the grating period, from Urata et al. (1998).*

$$\frac{dP_n}{d\Omega} = \frac{e\ I\ n^2 L}{2D^2\epsilon_0}\frac{\sin^2\theta\sin^2\phi}{(1/\beta - \cos\theta\ \sin\phi)^3}\ |R_n|^2 \times \exp\left(-\frac{d}{h_{int}}\sqrt{1+(\beta\gamma\ cos\phi)^2}\right) \qquad (2)$$

where e is the electron charge, I the beam current, L the grating length, ϵ_0 the permittivity of free space and d the distance of the beam above the grating. The Lorentz factor γ is given by $(1-\beta^2)^{-1/2}$.

The radiation factor $|R_n|^2$ is analogous to the reflection coefficients of optical gratings and is a measure of grating efficiency. Radiation factors can be computed following the modal expansion method of Van den Berg (1973) and Haeberle' et al. (1994) and are a function of beam energy and observation geometry. In the THz experiments being proposed here the radiation factors are ∼3.4 for a metallic grating and a 30 keV beam (Urata et al. 1998).

In our experiments we will use an electron beam generated by an SEM. At the brightness levels typical of such beams the SP radiation is in the *spontaneous* regime,

meaning that the radiation from the grating does not significantly impact the electron beam itself. The observed SP intensity is equal to the incoherent sum of the radiation induced by the interaction of electrons in the beam with the grating and is proportional to the beam current. Even at modest beam brightness the observed SP intensity can be an order of magnitude higher than that of a black body radiator at 3000 K (Kapp et. al. 2004). As described by Kapp et al., under certain conditions the image currents induced on the grating can interact with the beam causing the electrons to "bunch" along its length with the period length D of the grating. This electron bunching is similar to what occurs in a free electron laser (FEL) and in TWTs. In an FEL the bunching is induced by alternating transverse magnetic fields. In TWTs the bunching is induced by interaction of the electron beam with a slow moving electromagnetic wave (see below). As an electron bunch moves down a FEL or TWT its charge density continues to increase. Under these conditions a SP device is said to operate in the *amplified* or *super-radiant* regime, with the growth rate per unit distance given by (Kapp et al. 2004):

$$\mu_g = \frac{2\pi}{(\gamma\beta)^2}\left(\frac{I}{\lambda\ b\ I_A}\right)^{1/2} \qquad (3)$$

For centimeter size gratings and beam currents of $\sim$1 mA, the power gain expected at THz frequencies is of order 10^6 (60 dB) (Kapp et al. 2004) over the (nW) power level obtained in the spontaneous emission regime. Therefore, in the super-radiant regime SP effect devices should be capable of producing output power levels of $\geq$1 mW, comparable to an FIR gas laser and orders of magnitude greater than solid state devices. To date no groups appear to have unambiguously detected super-radiant emission using SP-effect devices at THz frequencies, most likely due to limited beam current and grating length (Urata et al. 1998; Knapp et al. 2004). **The detection and characterization of the super-radiant regime of an SP-effect device at THz frequencies will be a major goal for the proposed study**. The custom gratings needed for the investigations will be fabricated using a high precision milling machine in the PI's lab.

Recently, it has been observed (Smith et al. 2004) that enhanced diffraction occurs in the natural gratings that are formed by negative index material (NIM) prisms used to study NIM metamaterials. Smith et al. (2004) have used a split-ring resonator (SRR) structure embedded in negative-ϵ material in their work. Their observations suggest that SP-effect experiments with a NIM grating would uniquely enhance the SP-effect radiation. From the work of Yamaguti et al. (2002) it appears an order of magnitude improvement in output power may occur if photonic crystals are used. An illustration of the generation of SP-effect radiation using a NIM grating is shown in Figure 4. **We will systematically move from the reproduction of the classical experiment of Smith & Purcell (1953) to investigate 2-D and 3-D photonic crystal implementations of both positive and negative index material gratings.**

2.2 Traveling Wave Tubes

Traveling wave tube amplifiers are currently in use from below 1 GHz to $\sim$100 GHz and are capable of generating power levels from watts to megawatts. They are used in a wide variety of applications; including radar, communications

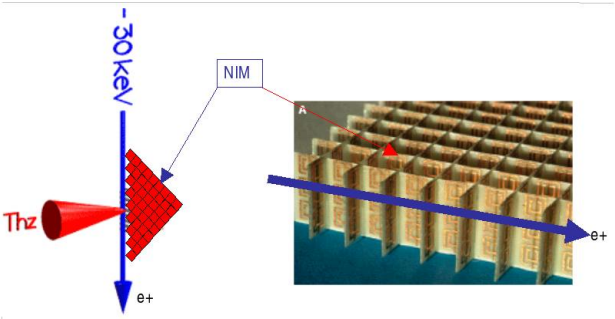

Figure 4: *Generation of enhanced SP-effect radiation from passing an electron beam to within close proximity of a negative index material (NIM) prism.*

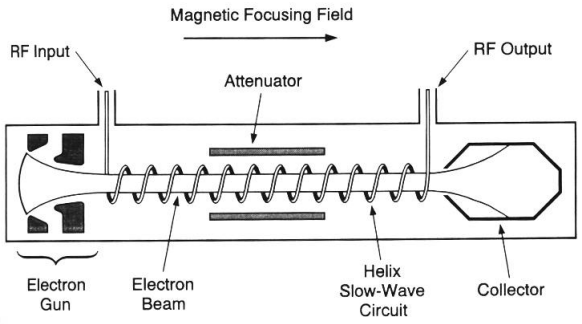

Figure 5: *Schematic of an experimental helical traveling wave tube (TWT), from Gilmour (1994).*

satellites, and electronic countermeasure systems. Amplification occurs through an interaction between an electron beam and a nearby radio frequency (RF) circuit carrying the signal to be amplified. Through the interaction some of the kinetic energy of the electrons in the beam is transformed into RF radiation. For this to occur the velocity of the RF signal flowing through the circuit must be slowed down to match the speed of the electrons in the beam. The possibility of such an interaction was recognized as early as 1933 (Haeff 1933). Lindenblad (1940) and later Kompfner (1942) were the first to describe using a helical transmission line wrapped around an electron beam as a tube architecture that meets these requirements. The helix serves as the slow-wave structure that matches the axial propagation velocity of the RF signal to that of the electron beam. The basic design of such a TWT is shown in Figure 5 (Gilmour 1994). Today slow-wave structures composed of coupled cavities also serve this purpose.

When an electron beam is injected along the axis of the helix axial electric field components of the RF signal accelerate some electrons while decelerating others. This interaction causes the electrons in the beam to bunch-up in a manner similar to that observed in the super-radiant regime of the SP-effect. As an electron bunch travels down the center of the helix each interaction with the RF signal increases the charge density in a given bunch. The fields produced by the bunching electrons in the beam will induce corresponding electric currents in the helix, adding constructively to the electric field of the signal it is carrying. As the beam-wave interaction continues, the induced waveform rapidly becomes larger than the initial signal and amplification occurs (Gilmour 1994). A figure illustrating the relationship between electron bunch charge density and RF circuit voltage with distance along the tube axis is shown in Figure 6 (Hess 1960).

Note that near the end of the tube the charge density in an electron bunch becomes large enough for space-charge forces to begin to disperse it, leading to destructive interference and field saturation.

Today the two most common types of slow-wave structures used are the venerable helix and coupled waveguide cavities. The helical design can generate tens to hundred of watts over as much as two

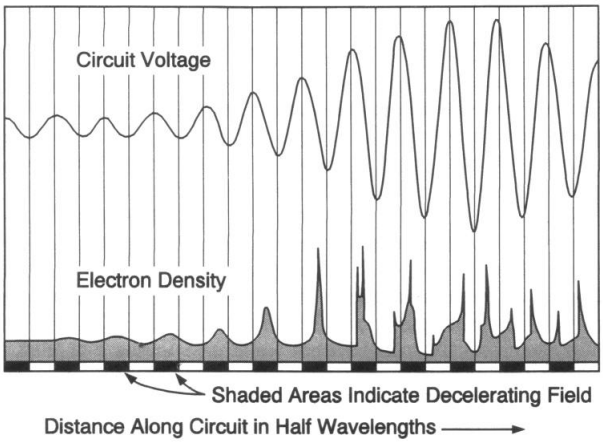

Figure 6: *Illustration of the interaction between electron beam and RF signal in a TWT, resulting in RF amplification. Adapted from Hess (1960) in Gilmour (1994).*

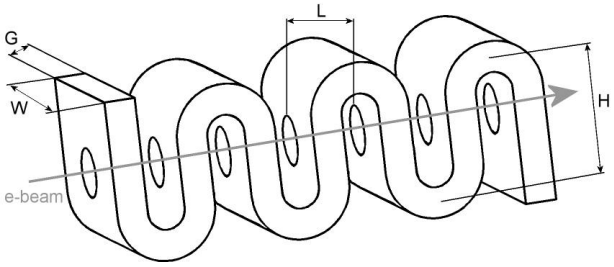

Figure 7: *3-D rendering of the geometry of a meandering waveguide slow-wave structure.*

octaves of frequency. The coupled-cavity type TWT is narrower band (10-20%), but is capable of producing megawatts of power. The practical high frequency limit of TWT's was continuously pushed to higher frequencies until the early 1990's when high frequency, high electron mobility transistors (HEMTs) became available. Today, HEMT-based amplifiers have been built to ∼200 GHz, beyond which limitations in photolithographic processing make them extremely difficult (or impossible) to produce. **The high frequency limit of TWTs is set principally by losses in the slow wave structure. Using modern machining and photolithographic techniques TWT operation to several THz should be possible. This plus the fact that TWTs have been shown to be capable of very low-noise operation (<0.2 dB, Hammer and Wen 1964) provides a strong incentive to push TWT technology to higher and higher frequencies.**

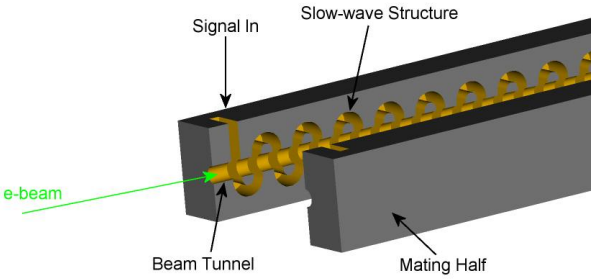

Figure 8: *3-D rendering of the proposed meandering waveguide structure to be implemented in a copper split-block first at 350 GHz and then at 1.5 THz.*

The implementation of a helical slow-wave structure becomes more difficult with frequency. Meandering waveguide has been successfully used at high frequencies as an alternative slow-wave structure (Figure 7). Here interaction between beam and wave is maintained by periodically folding the waveguide back into the beam path. Sharp corners in the bends should be avoided in order to reduce reflection which reduce gain. The waveguide cross section should be retained in the bends for the same reason. Electron-signal interaction occurs where the particle beam passes through the waveguide. The degree of electron-beam interaction that takes place at each encounter is described by the gain parameter C, given by (Pierce 1950):

$$C = \left(\frac{Z_\circ}{4\, V_\circ / I_\circ} \right)^{1/3} \tag{4}$$

where $Z_\circ$ is the interaction impedance and $V_\circ/I_\circ$ is the beam impedance. Waterman (1979) successfully constructed a 46 GHz TWT using the meandering waveguide structure shown in above. For this structure he derives a value of $Z_\circ = 4.65\Omega$. For our proposed investigations we will use a $1/8^{\text{th}}$ scale of Waterman's design implemented in a copper "split-block" (J. Waterman has agreed to collaborate with us on this project, see Support Letter). A 3-D rendering of the machined structure is shown in Figure 8. At the design frequency of 368 GHz the characteristic dimensions of the meandering structure are $G = 79.5$ μm, $W = 457$ μm, $L = 177$ μm , and $H = 346$ μm, with a 127μm diameter beam hole. With our electron microscope beam source (see discussion below), typical values of beam current and voltage are $V_\circ = 25$ keV and $I_\circ = 1$ mA. Substitution into the above equation then yields a value of $C = 0.0036$. The power gain P_G of a TWT can be expressed as (Gilmour 1994):

$$P_G = 47.3\, CN \,\text{dB}$$

where $N = \text{tube length}/L$. To achieve a value of P_G of 10 dB will require a $N \sim 59$ and an overall tube length of ~ 1 cm. Empirical measurements (Kapp et al. 2004) of the growth of a similar electron beam over this distance yielded an average beam diameter of $\sigma = 42$ μm. This value of sigma is less than $1/4^{\text{th}}$ the diameter of the beam hole, indicating the beam will remain sufficiently collimated throughout the structure, obviating the need of an additional collimating magnetic field. Clearance of the beam through the tunnel will be monitored by precisely measuring the temperature of the waveguide block. An accidental encounter of the beam with the block will raise the block's physical temperature. Using the precision milling machines available in the PI's lab (see below), the slow-wave structure can be fabricated with surface finishes approaching optical quality, minimizing waveguide loss. We have modeled the full length of the slow-wave structure in CST Microwave Studio and found the total loss (including the effects of finite conductivity, surface roughness and leakage through the beam tunnel) to be ≤ 2 dB across the operating range of the tube (Figure 9).

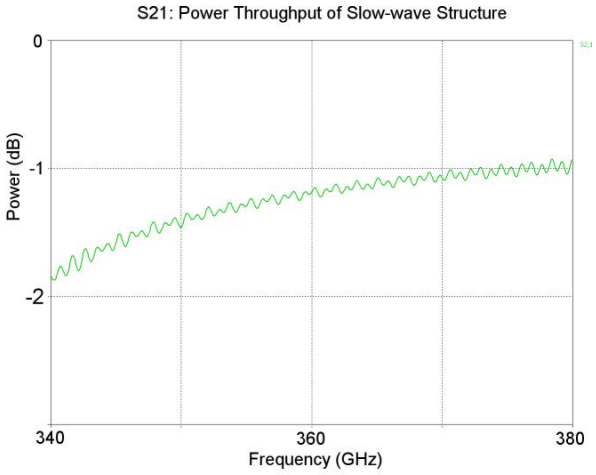

Figure 9: *CST Microwave Studio simulation of the proposed design demonstrates low losses across the full operating range of the TWT.*

Predictions of C, $Z_\circ$, and P_G will be tested by real circuits and beams in experiments with the modified SEM. Experimentally-determined coupling impedances will then be used in large-scale TWT simulations (from Raytheon) to design optimized TWT circuit lengths and parameters. TWTs below 30 GHz routinely have 60 dB of power gain, so there is good reason to hope for a successful outcome. Once a TWT has been successfully demonstrated (i.e. exhibited a

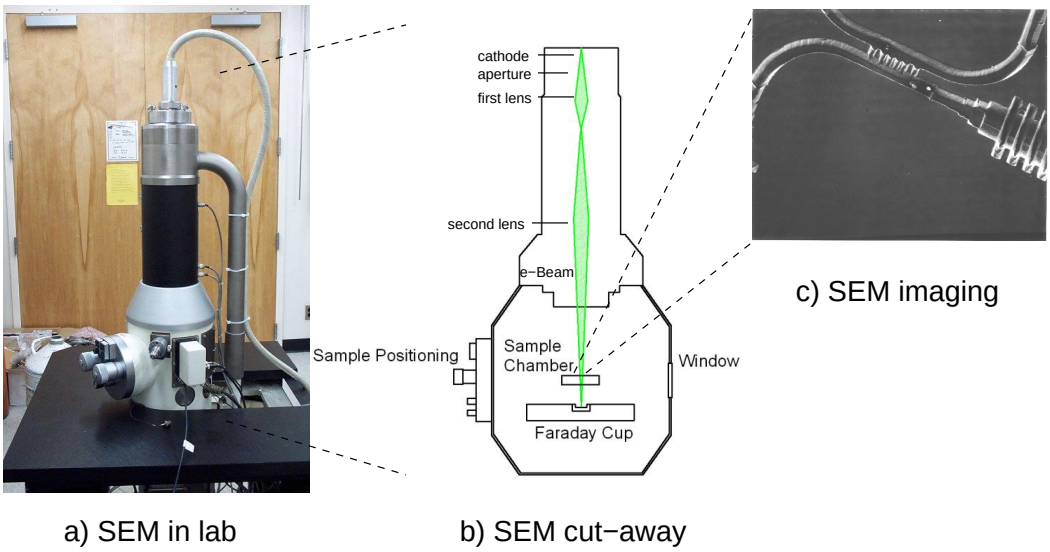

Figure 10: *a) The Amray™1000a scanning electron microscope in the PI's lab. b) Cutaway diagram of the SEM. c) Image of the branch-line coupler in Figure 13 taken with the Amray™ SEM.*

predictable amount of gain) at 368 GHz, a THz version of the device will be designed and constructed.

In the implementation of a new TWT amplifier undesired backward wave oscillation (BWO) may occur, turning the amplifier into a source of coherent radiation. BWO's can be significantly reduced or eliminated by severing the slow-wave circuit. The two halves of the slow-wave circuit remain reconnected by the electron beam which then induces an amplified version of the input signal in the second half of the circuit. If undesired BWO's are found to be present in the output of the 368 GHz tube, we will add a sever. However, as described above, there are many applications where a clean source of coherent THz radiation is desirable. Therefore, as part of our investigation, we will optimize a tube design to act as a BWO.

3 Experimental Approach

In the past, development efforts in SP-effect and TWT devices have been out of reach of most university investigators due to the lack of a flexible electron beam source. John Walsh's group at Dartmouth were the first to use an SEM to characterize electron beam devices (Urata et al. 1998). Both proposed SP-effect and TWT test setups will utilize a recently refurbished, Amray™1000a Scanning Electron Microscope. A picture of the unit in the PI's lab is shown in Figure 10a. Figure 10b is a schematic of the SEM's magnetic lensing system. Figure 10c is an image obtained with the SEM of a 1.45 THz waveguide structure machined in the PI's lab. The Amray 1000a can be configured either as a narrow beam, high magnification SEM or as a somewhat broader ($\Omega \sim 50$ μm) higher beam current (~ 1 mA) source. The configuration change can be made in a matter of minutes.

The availability of an SEM as a flexible e-

beam source is an invaluable tool for the proposed work.

3.1 Smith-Purcell

The experimental set-up for characterizing SP-effect devices is shown in Figure 11. The SP-effect grating is oriented in the sample chamber such that the e-beam travels just above and transverse to the grating's grooves. Even with apertures removed in the focusing optics to permit higher current operation, the SEM can provide images of sufficient resolution to orient the beam relative to the grating. The beam focus is placed midway along the grating. The test set-up must provide a means of coupling SP-effect radiation from the grating to outside the SEM's sample chamber. In a series of experiments resulting in the measurement of spontaneous SP-effect emission, Kapp et al. (2004) used a hollow brass pipe to convey some fraction of the emitted radiation to a vacuum window. We will initially adopt a similar approach here. The emerging radiation will be synchronously detected by an Infrared Lab's 4°K bolometer system. Power measurements will be made both as a function of beam impedance and grating orientation. As part of the device characterization, the power pattern of the emergent beam will be measured. The temperature grating block will be monitored with the goal of detecting when the e-beam inadvertently strikes the grating. Temperature monitoring will have the added benefit of allowing the blackbody contribution to the emitted radiation to be estimated. The grating will also be electrically isolated so the beam current striking it can be measured. Based upon measurement results, the grating design will be re-optimized, machined, and characterized in the PI's lab.

3.2 TWT

The experimental set-up for TWT characterization is provided in Figure 12. The meandering waveguide, slow-wave structure is oriented vertically in the sample chamber so the e-beam can enter the beam tunnel. The e-beam focus is placed midway down the structure. Images will be made with the SEM to help align the TWT with respect to the beam. Input and output signals are coupled to the TWT via waveguide flanges. At 368 GHz, a solid-state source comprised of a Gunn oscillator and frequency multiplier provides the input signal to be amplified. An existing Coherent-DEOS laser will provide the 1.5 THz input signal for the second-generation TWT devices. Two directional couplers with power detectors are used on the input and output in order to provide an accurate measurement of power gain. Both input and output signals will be coupled via waveguide to the sample cell. As in the case of the SP grating, the waveguide block will be both electrically isolated and instrumented with a sensitive temperature sensor in order to detect the charge or heat of the electron beam if it strikes the block. The TWT's performance will be measured as a function of frequency and beam impedance. New slow-wave structures will be designed and fabricated as needed. The test set-up of Figure 12 can also be used to characterize a TWT structure designed to operate as a BWO. In this case the BWO output port is actually near the beam entrance; the other waveguide waveguide board would be terminated.

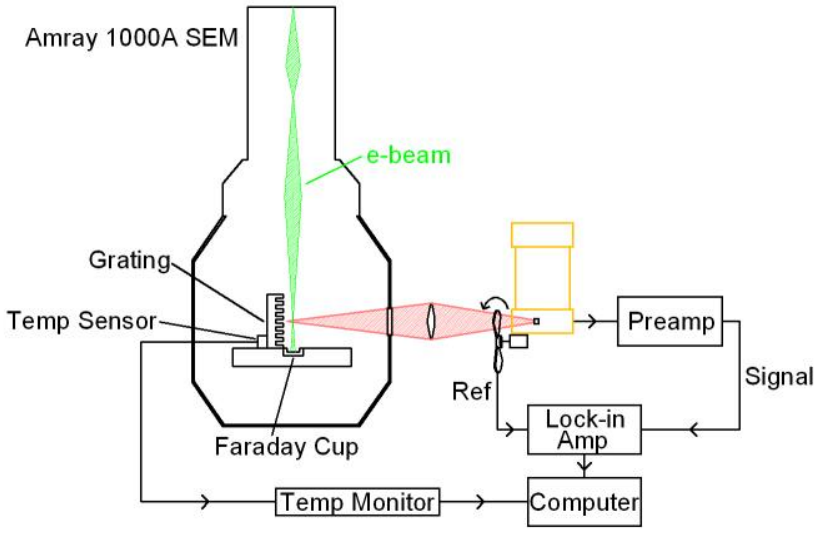

Figure 11: *Experimental schematic for characterizing Smith-Purcell effect devices.*

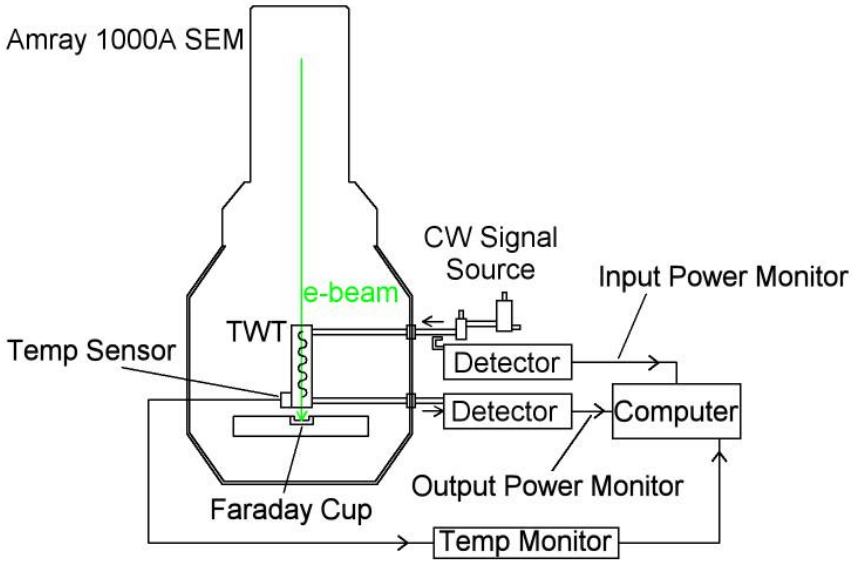

Figure 12: *Experimental schematic for characterizing traveling wave tube (TWT) devices.*

4 Precision Micromachining

Both the SP-effect gratings and the TWT slow-wave circuits have structures that are small compared to the design wavelengths. The ability to machine such structures at the required size scale and accuracy has been a major hurdle in scaling well–characterized structures from the microwave to THz spectral regimes. With the aid of funds from the NSF, NASA, and Army Research Office over the past decade, the PI's group at the University of Arizona has established a micromachining capability uniquely suited to making high quality waveguide and quasi-optical components to (sub)micron accuracies. The lab contains two custom-designed laser micro-

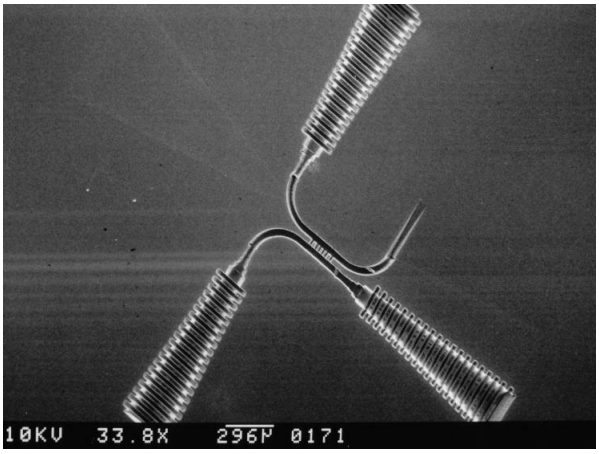

Figure 13: *SEM imaging of a 1.5 THz branchline coupler based on the Atacama Large Millimeter Array (ALMA) design, fabricated using the laser micromachining system at the University of Arizona.*

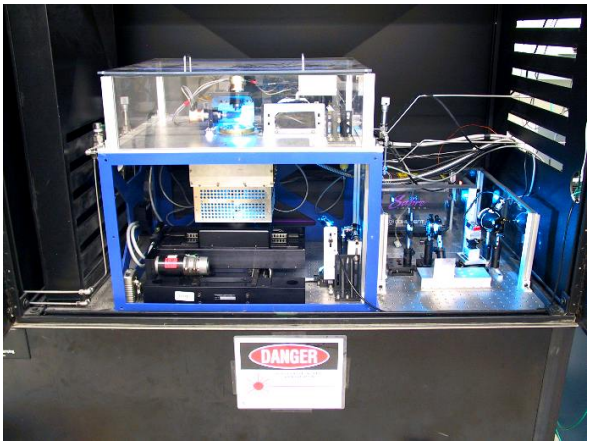

Figure 14: *Laser micro-milling machine in the PI's laboratory, used for fabrication of devices at frequencies >1 THz.*

machining systems. One system is optimized for making waveguide devices from $\sim$ 0.8 to 5 THz. The second system is used to make similar devices from $\sim$ 5 to 30 THz. In these systems the beam from an argon-ion laser is focused onto a silicon wafer residing in a 200 Torr chlorine ambient. The incident laser beam has enough power (typically several watts) to vaporize a small volume ($\leq 1\ \mu m^3$) of silicon that reacts with the chlorine to make $SiCl_4$, which remains in the gas phase. Under computer control the laser beam can be steered to create 3-D structures such as gratings or meandering waveguides (d'Aubigny et al. 2004). Once the etching is complete, the etched silicon is gold plated as needed to make it behave like normal waveguide or quasi-optical structures. An example of a 1.5 THz waveguide power combiner fabricated with the system is shown in Figure 13. A picture of one of the laser micromachining systems to be used for the THz portion of the proposed work is shown in Figure 14.

At frequencies below 1 THz the size of the structures to be etched often require volumetric removal rates beyond the capabilities of the laser micromachining systems. In order to fabricate such structures the PI's group has recently obtained funds from the NSF's MRI program to procure a state-of-the-art micromilling machine (KERN MMP 2522, see Figure 15) that can machine metallic and ceramic structures to 1 micron precision and accuracy. This system will be used to machine prototype 345 and 368 GHz SP-effect gratings and TWT slow-wave structures for the proposed effort, whereas the laser micromachining system will concentrate on fabrication of the 1.5 THz structures.

The availability of these systems will permit the rapid prototyping and optimization of the gratings and waveguide components needed for this project, from microwave to THz spectral regimes.

5 Realizing Practical Devices

The primary goal of the proposed work is to demonstrate TWT and SP-effect devices at THz frequencies. Using the

Figure 15: *Kern micro-milling machine in the PI's laboratory, used for fabricating devices at frequencies < 1 THz.*

e-beam of an SEM provides the most flexible and readily-available means for achieving this goal. However, to make these devices practical they must be designed to operate in compact, efficient, self-contained packages. Once we have experience operating these devices at THz frequencies, we will be better able to optimize their operating characteristics. The main task will then be to design a new cathode based on low-power, low-temperature field emitters such as carbon nanotubes. Cathodes employing carbon nanotubes have already been demonstrated in a Northrop/Grumman TWT at 4.5 GHz (see Figure 16) and require only 250V of gate voltage. At THz frequencies the size of a unit such as this can be reduced by an order of magnitude, making them very attractive for space-based applications as well. Carbon nanotubes may have the additional advantage of having exemplary noise performance. In 1964, Hammer & Wen found that high-B fields applied in the vicinity of the cathode reduced the transverse velocity component in the e-beam, significantly improving the noise performance of the TWT. Therefore nonthermionic emitters such as carbon nanotubes may intrinsically provide better noise performance. **In the third year of the proposed effort we will perform a detailed design study of an SP-effect and TWT device that is optimized for use with field emission devices.**

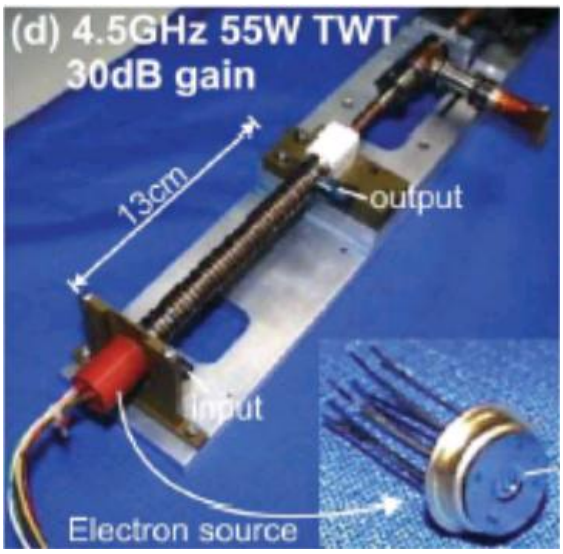

Figure 16: *Milne et al. (2003) demonstration of compact TWT and electron sources at 4.5 GHz using carbon nanotube technologies. This example showcases the kind of packaging we will explore at 350 GHz and 1.5 THz.*

6 Plan of Action

Year 1

1. Upgrade SEM to operate at high currents & voltages
2. Complete assembly of test bed electronics

3. Design and fabricate SP-effect grating and coupling optics optimized for 350 GHz
4. Design and fabricate TWT slow-wave structure optimized for 350 GHz
5. Perform initial experiments with SP-effect grating in spontaneous emission regime
6. Perform initial experiments with TWT slow-wave structure

Year 2

1. Make necessary design changes to SP-effect grating & optics and TWT structure based upon Year 1 results
2. Repeat performance tests using reoptimized structures
3. Design SP grating structures using photonic crystal and NIM material
4. Test performance of SP-effect grating in super-radiant regime
5. Test performance of TWT in backward-wave oscillator (BWO) mode

Year 3

1. Test performance of photonic band gap and NIM-based SP grating
2. Design, fabricate and test SP-effect grating for operation at 1.5 THz
3. Design, fabricate and test TWT slow-wave structure at 1.5 THz
4. Perform a design study for implementing THz SP-effect signal sources and TWT amplifiers as standalone, compact units

7 Educational Impact

The Astronomy, Optical Sciences, Electrical Engineering, and Physics Departments at the University of Arizona and Raytheon Inc. are teaming together to create a Center of Excellence in THz Science & Technology. The purpose of the center is to 1) contribute to breakthroughs in the THz spectral regime and 2) train students in the multidisciplinary approach to the formulation and solving of problems. Students must learn this approach if they are to play a leadership role in today's research environment. The proposed investigation is an ideal match to these goals.

The design, fabrication, and test of SP-effect and TWT devices will be the focus of the dissertation work of at least two graduate students and the senior research projects for two undergraduates. In addition, 2 or more engineers and/or physicists from Raytheon Inc. are expected to participate in the proposed research and use it to help fulfill requirements for advanced degrees. As part of our collaboration, Raytheon is interested in employing undergraduates for summer intern positions in related fields. The exposure students will receive to the corporate research environment will help them in making career choices in the future. The PI has faculty appointments in Optical Sciences and Electrical Engineering, as well as Astronomy. These appointments enable him to serve as the graduate advisor to students in all three departments. Currently he is the thesis advisor to 3 Ph.D. students in Astronomy, 2 Ph.D. students in ECE, and 1 Ph.D. student in Optical Sciences. Three undergraduate (1 Physics, 2 Optical Sciences) are now employed in the PI's lab.

8 Results from Prior NSF Support

- A NSF Young Investigator Award (AST-9457445) was made to the PI for the period 7/1/94 - 7/1/99 of $62,500 per year (matching funds have been obtained for all 5 years). This award was used to support research and teaching efforts. Research included further development of the laser micromachining waveguide technology, the construction of submillimeter receiver systems and/or components at 230, 345, and 490 GHz for the Heinrich Hertz Telescope (HHT), a 492/810 GHz receiver system for the AST/RO telescope at the South Pole, the funding of graduate and undergraduate students for the study of protostellar evolution, and the construction of a submillimeter polarimeter and student radiotelescope. The receiver systems described above are (except for the polarimeter) facility instruments. We estimate $\sim$30 papers from the HHT and 20 papers from AST/RO contain observations made with these instruments. Papers describing the instruments are Groppi et al. 2000; Walker et al. 2001).

- A grant (AST-9622569) from the NSF ATI program was made to the PI to construct the 7-channel, 345 GHz array (DesertSTAR I) for the HHT. (formal title: "An 870 micron Array Receiver for the Heinrich Hertz Telescope") The award period was from 8/1/96 - 7/31/99 for a total of $380,931. DesertSTAR has been a successful collaboration between the University of Arizona (PI: system design and construction), NRAO (John Payne: J-T cooler), the University of Massachusetts (Gopal Narayanan and Neil Erickson: mixers and LO), and the University of Virginia (Art Lichtenberger: SIS junction fabrication). It will be the first array receiver to operate in the 870 micron atmospheric window (Groppi et al. 2000; 2003).

- An award (ECS-9800260) from the NSF Physical Foundations of Enabling Technologies Program was made to the PI to construct and utilize a laser micromachining system at the University of Arizona (Drouet d'Aubigny et al. 2001). The award period was from 6/1/98 - 5/31/00 for a total of $280,000. The system is fully operational and has been used to make waveguide components for integrated array development and prototype quasi-optical structures for NASA's *Terrestrial Planet Finder*.

- A grant from the NSF ATI program was awarded to the PI and Co-I Daniel Prober (Yale University) to develop "An Integrated 370 micron Heterodyne Imaging Array". This is an ongoing effort to combine laser micromachining technology with recent developments in Hot Electron Bolometer (HEB) mixers to develop the first truly integrated submillimeter-wave heterodyne imaging arrays (Groppi et al. 2002). The arrays are being designed to permit scaling to higher frequencies and formats. The award amount ($450K) is being divided over a three year period (02/01/02 to 01/31/05) between the participating institutions.

- A subaward of $99,348 was provided to the PI from the NSF ATI program for his contribution to "A 1.5 THz Common User Receiver System" (S. Yngvesson- PI). Over the two year award period (01/01/00 to 12/31/02) the PI's group designed and built the cryogenic, electronic, and optical system for the TREND 1.5 THz receiver system now on the AST/RO telescope at the South Pole. The laser LO system and high frequency mixer were provided by the University of Massachusetts (Gerecht et al. 2003).

- A subaward of $290K from the NSF Office of Polar Programs was made to the PI for his group's work in "Continuing Operation of the Antarctic Submillimeter Telescope and Remote Observatory" (A. Stark- PI: OPP-0126090). The PI's group built most of the facility receivers for AST/RO. This 3 year award (02/01/02 to 01/31/05) supports the continued maintenance and upgrade of these systems (Stark et al. 2001).

- An MRI award of $1,742,356 was made to the PI from the ECS division to construct "SuperCam: A SuperHeterodyne Camera for the Heinrich Hertz Telescope" (AST-0421499). The PI's group is in the first year of a 3 year proposal to build the worlds first large format, submillimeter-wave heterodyne receiver system. SuperCam will contain 64 independent receiver pixels. The instrument will reside on the Heinrich Hertz Telescope and be used to map the plane of the Milky Way and nearby galaxies in a variety of important astrophysical emission lines. The duration of the award is 09/01/04-8/31/07.